High-Power Ultrawideband Radiation Source with Multielement Array Antenna

V.I. Koshelev, V.P. Gubanov, A.M. Efremov, S.D. Korovin, B.M. Kovalchuk, V.V. Plisko, A.S. Stepchenko, K.N. Sukhushin

Institute of High Current Electronics, RAS, 4 Akademichesky Ave., Tomsk, 634055, Russia
Phone: +7(3822)491915, Fax: +7(3822)492410, E-mail: koshelev@lhfe.hcei.tsc.ru

Abstract – The paper presents results of investigations of gigawatt-power level ultrawideband (UWB) radiation sources based on a multielement array and a single antenna.

1. Introduction

UWB radiation sources with the peak power of ~ 10^{10} W are necessary for solving a number of tasks. Creation of this type of sources is possible on the basis of multielement arrays with the peak radation power of a single array element equal to 0.1–1 GW. Results of our previous investigations in this direction are presented in [1–3]. The aim of this work was to increase the peak radiation power of a single antenna source up to 1 GW as well as to develop and investigate a multielement array source.

The external view of the array antenna source is presented in Fig. 1. The source includes a generator of monopolar pulses (GMP) 1, a bipolar pulse former (BPF) 2, a wave transformer (WT) 3 and a rectangular 16-element array 4. The array elements are connected to the transformer output with cable feeders. In the single antenna source, the transmitting antenna was connected with BPF by means of a coaxial feeder. Short description of the design and investigation results of both separate components and sources as a whole are presented below.

2. Generator of Bipolar Pulses

A generator of monopolar pulses "SINUS-160" analogous to the one described in [3] was used as a source of a pulse line charging of BPF. As distinct from [3], charging voltage of the GMP forming line is increased to 360 kV.

Figure 2 presents the equivalent BPF scheme. The scheme includes four coaxial lines FL0–FL3, a sharpening S1 and a crow-bar S2 discharge switches, separating inductor with inductance L = 250 nH and a load RL. The lines FL0–FL2 have electric length τ = 0.35 ns and wave impedance ρ = 25 Ohm.

The transmitting line FL3 with a 3.7-ns electric length is matched with the load $RL = 2\rho = 50$ Ohm. The forming line FL0 is charged from GMP through the charging inductor L up to the voltage $-U_0$. At operation of the sharpening discharge switch S1, a negative pulse of the amplitude $-U_0/2$ is propagating by the line FL1 that is loaded at the end with the lines FL2 and FL3 connected in series with the common impedance of 3ρ. Voltage wave passing into the line FL3 is forming at the load a negative half-wave of a bipolar pulse with the amplitude of $-U_0/2$. In the 2τ time, when a reflected wave reaches the beginning of the line FL1 and the wave passing into FL2 reaches its end the crowbar discharge switch S1 will operate. Now, the positive wave of the voltage removal propagates along the line FL1 and the double positive wave reflected from the opened end propagates along the line FL2.

These two waves come to the output FL1 and input FL2, add together and form at a load a positive bipolar pulse half-wave with the amplitude $U_0/2$. In the time

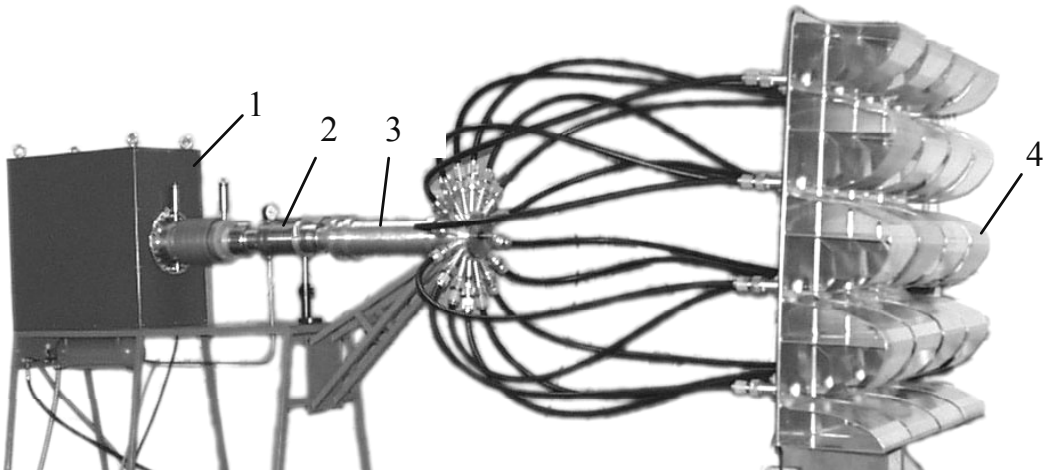

Fig. 1. External view of the source with array antenna

4τ the transient process is over. Hence, at the ideal commutation of the discharge switches S1 and S2, a bipolar pulse with the amplitude ± U_0/2 and the length of 4τ appears at the load.

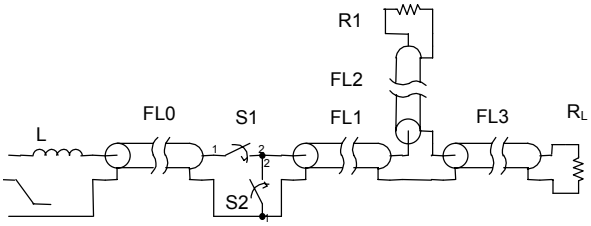

Fig. 2. Equivalent BPF scheme

The BPF scheme was simulated at a personal computer by the program PSpice. The commutation time, i.e., the time during which the discharge switch resistance changes from 100 kOhm to 0.01 Ohm is determined to be equal to 1 ns for S1 and S2.

A 1000-kOhm resistor R1 is necessary only to provide calculation. The charge inductance value L was chosen so that it should provide at the line FL0 the charging voltage close to maximum at the minimum charging time. Maximum charging voltage at the forming line FL0 reaches 555 kV during the time of ≈ 5 ns. When the dischrge switch S1 operates near the charging voltage maximum and S2 operates with a relative delay of 0.7 ns, then a bipolar voltage pulse with the amplitudes of ≈ 270 kV and length of ≈ 1,8 ns is formed at the load (Fig. 3).

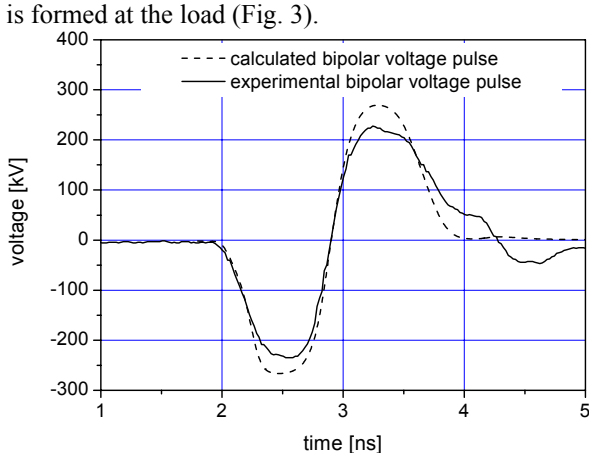

Fig. 3. Voltage pulse from BPF output

A BPF design presented in Fig. 4 consists of gas and oil volumes divided by the feed-through caprolon insulators. The charging inductor L, four coaxial lines FL0-FL3, sharpening S1 and crowbar S2 discharge switches are placed inside the case in nitrogen medium under the pressure of 7–9 MPa. The internal conductor diameters of the lines FL0–FL2 are equal to 33, 33 and 16 mm, respectively. The line FL2 has Teflon 4 insulation. The ends of the internal conductors of the lines FL0 and FL1 are the electrodes of the sharpening discharge switch S1 and a 2-mm thick disc and insertion at the external conductor of the lines FL0 and FL1 are the electrodes of the crowbar discharge switch S2. The discharge switch electrodes are made of copper.

The transmitting line FL3 connects the BPF output either with the resistive load or with the single antenna. They are not presented in Fig. 4. The right and left parts of the line FL3 have gas and oil insulations, respectively. The voltage pulse signal from the BPF output was recorded with the oscillograph TDS7404 by means of the voltage devider on the coupled lines D [4] installed inside the oil-filled line FL3.

At the nitrogen pressure of 9 MPa in the BPF volume and the gaps in the discharge switches S1 and S2 equal to 1.4 and 1.2 mm, respectively, the output voltage signal from the BPF depicted in Fig. 3 has approximately equal amplitudes at a 230-kV level. The crowbar discharge switch operates in conditions of high voltage rise rate at the electrodes ~ 5 · 1014 V/s and multichannel commutation mode with subnanosecond time and high stability is realized. Relative voltage amplitude spread doesn't exceed 3% of RMS. Owing to erosion of discharge switch electrodes, stability decrease and pulse shape distortion were observed in 1–2 hours of operation with the pulse rate of 100 Hz. Pressure decrease in the BPF by the value of ~ 0.5–1 MPa results in stability and pulse shape recovery and increase of the BPF operation time up to 5 hours without changing the electrodes.

The wave transformer was used to match the BPF wave impedance of 50 Ohm and the summary wave impedance of the array antenna feeder of 3.125 Ohm. The WT design presents a 650-mm long oil-filled coaxial, its wave impedance ρw being changed along z-axis by the law $\rho w = 50\exp(-4.62z)$. Diameters of

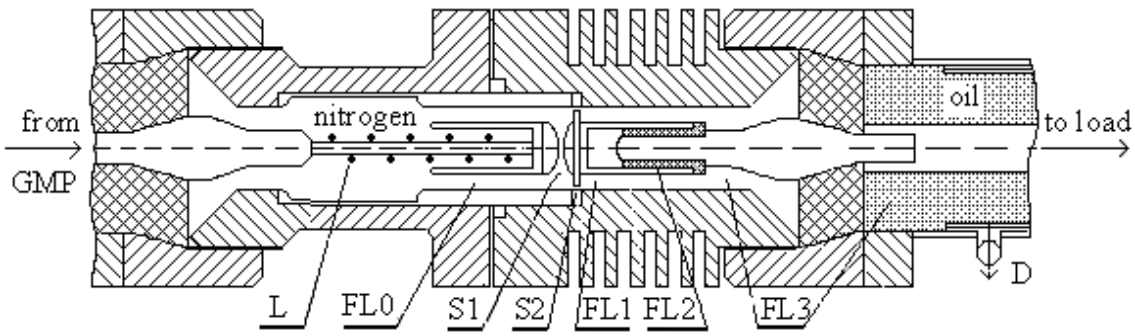

Fig. 4. BPF design

the external conductors at the coaxial input and output are equal to 65 and 120 mm, respectively. The wave transformer input is connected to the BPF output without the oil-filled line FL3 and the output is connected to the array antenna with the cables PK-50-17-17. To record the output pulse from the WT, a capacitive voltage divider is installed in one of the cables. Fig. 5 presents the calculated and measured pulses at the WT output.

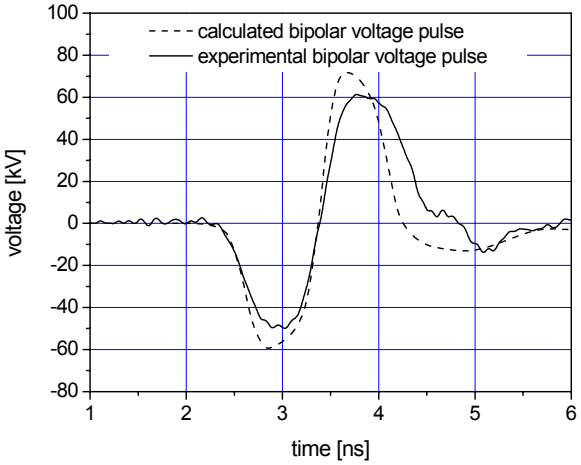

Fig. 5. Voltage pulses at WT output

3. Transmitting Antennas

To radiate UWB electromagnetic pulses, a single combined antenna and a 16-element array antenna were used.

In the presented UWB sources a modified variant of antenna described earlier in [5] was used. The antenna is a combination of an electrical monopole, two magnetic dipoles and a TEM-horn. In order to prevent breakdowns, the single antenna is placed into a thin-walled polyethylene container filled with SF_6-gas up to the pressure of 0.15 MPa.

Figure 6 presents the combined antenna VSWR versus frequency in the dielectric container and without it. As it is seen from the figure, the container insignificantly effects the antenna matching with the feeder having the wave impedance $\rho_f = 50$ Ohm. In the frequency band of 0.2÷1 GHz, where the main part of a 2-ns long bipolar pulse energy is concentrated, VSWR $i_s < 3$.

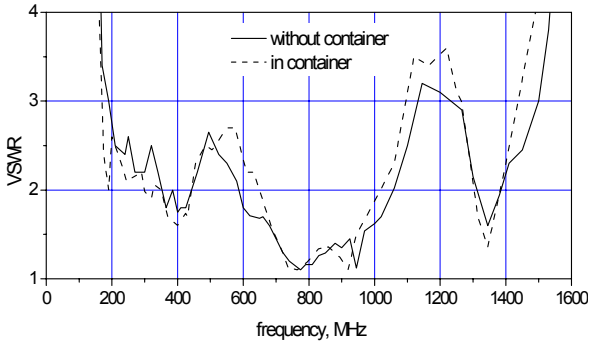

Fig. 6. Transmitting single antenna VSWR

Detailed measurements of spatial-temporal radiation characteristics were carried out only at the antenna excitation with a low-voltage bipolar pulse. The width of the antenna pattern for a vertically polarized electric field by the half peak power level is 90° for the *H*-plane and 80° for the *E*-plane. In the *E*-plane, the antenna patern is nonsymmetric relative to the plane $\delta = 0°$ and its maximum is placed under the angle $\delta = 7°$. Power level of the cross-polarized radiation in the *E*- and *H*-planes doesn't exceed 5% of the maximum power level for the vertically polarized radiation.

At the antenna excitation with a 2-ns long bipolar pulse, the reflected energy was equal to ~ 10% of the bipolar pulse energy.

The antenna efficiency by energy (~ 90%) and spatial-temporal radiation characteristics being known, we can find the antenna effiiency by the peak power $k_p = P_r/P_g$, where P_r is the peak power in the antenna radiation pulse, P_g is the peak power in the voltage pulse at the antenna input. Measurements carried out at the antenna excitation with a 2-ns long low-voltage bipolar pulse gave the value $k_p \cong 1.2$. The measured antenna directivity was $D = 5.5$. From here, we can find the peak electric field strength at a distance R:

$$E_P(R) = \frac{1}{R}\sqrt{30 P_g k_p D}\,, \qquad (1)$$

where $P_g = U^2_p/\rho_f$, U_p is the generator voltage pulse amplitude.

Using (1), the figure-of-merit equal to the product of the peak field strength multiplied by the distance E_pR can be found. The peak field strength in the measurements was determined from the ratio

$$E_p(R) = \frac{U}{h_{ef}}\,, \qquad (2)$$

where U is the maximum voltage at the receiving antenna and a hef is the efficient height of the receiving TEM-antenna [3] determined in accordance with [6].

The array antenna consists of four vertical sections with four radiating elements in each fastened at a dielectric plate. Each radiating element presents a previously described combined antenna. The neighboring elements in the vertical section are coupled galvanically with each other while the sections are not coupled galvanically. As it is shown in [5], this design allows minimizing VSWR of the array elements.

VSWR for the array elements are shown in Fig. 7. Curve 2 is the VSWR of the cone upper elements and curve 1 is the typical VSWR for all the rest elements. It is seen from the plots that VSWR became smoother and in the region of 200–800 GHz it even decreased in comparison with a single antenna.

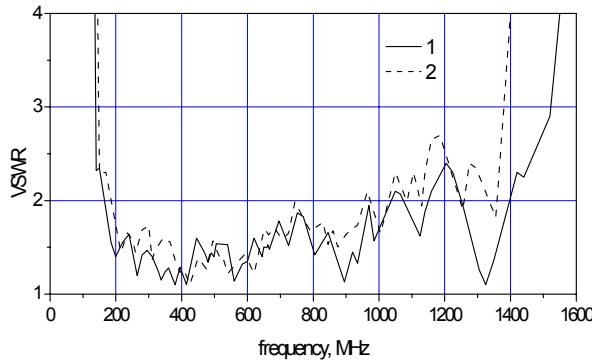

Fig. 7. VSWR of array elements

The energy reflected from the array element at the excitation with a 2-ns bipolar pulse made up 6–7%. During measurements, all antennas except the tested one were connected to the matched load.

4. Experimental Investigations

Figure 8 presents the pulse radiated by the single antenna excited with a high-voltage pulse. The peak field strength measured at the distance $R = 9$ m from the transmitting antenna is $E_p \cong 56$ kV/m. Voltage pulse amplitude of a high-voltage generator $U_p = 230$ kV and previously obtained values $k_p = 1.2$ and $D = 5.5$ being known, the peak strength of the field at a distance $R = 9$ m that equals to $E_p \cong 50$ kV/m will be calculated. The obtained values of E_p differ by ~ 10%.

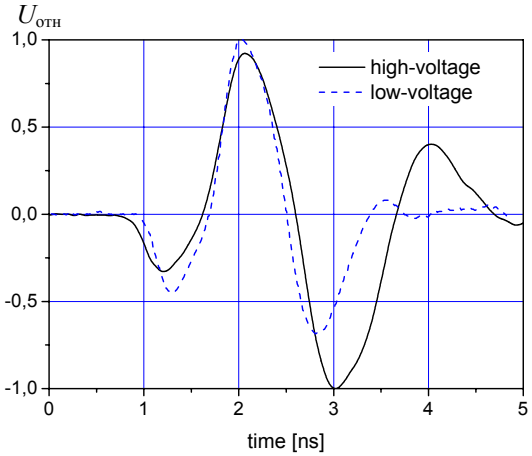

Fig. 8. Waveforms of combined single antenna radiation pulses

It follows from the obtained value of $k_p = 1.2$ that at a 230-kV bipolar pulse amplitude, vertically polarized radiation peak power is ~ 1.2 GW.

Figure 9 presents the waveform of the pulse radiated by the array excited with a high-voltage pulse.

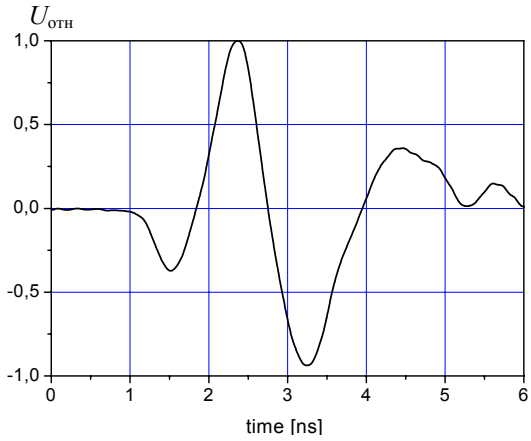

Fig. 9. Waveform of array radiation pulse

The measured figure-of-merit is $E_pR \cong 1670$ kV.

5. Conclusion

Gigawatt-power level sources of UWB radiation were developed on the basis of the multielement array and single antenna withnthe pulse repetition rate of 100 Hz. Antenna array application allowed decreasing the pattern width by ~ 4 times and increasing the field strength by ~ 3.3 times.

The authors are thankful to G.A. Mesyats for support of the work and to Yu.A. Andreev and S.E. Shipilov for assistance.

References

[1] V.I. Koshelev, Yu.I. Buyanov, B.M. Kovalchuk, Yu.A. Andreev, V.P. Belichenko, A.M. Efremov, V.V. Plisko, K.N. Sukhushin, V.A.Vizir, V.B. Zorin, *in: Proc. SPIE*, 1997, pp. 209–219.

[2] Yu.A. Andreev, Yu.I. Buyanov, A.M. Efremov, V.I. Koshelev, B.M. Kovalchuk, V.V. Plisko, K.N. Sukhushin, V.A. Vizir, V.B. Zorin, *in: Proc. 12th IEEE Int. Pulsed Power Conf.,* 1999, pp. 1337–1340.

[3] Yu.A. Andreev, V.P. Gubanov, A.M. Efremov, V.I. Koshelev, S.D. Korovin, B.M. Kovalchuk, V.V. Kremnev, V.V. Plisko, A.S. Stepchenko, K.N. Sukhushin, Laser and Particle Beams **21**, 69 (2003).

[4] A.M. Efremov, B.M. Kovalchuk, Pribori I Technika Experimenta **6**, 69 (2004) (Rus).

[5] V.I. Koshelev, Yu.I. Buyanov, Yu.A. Andreev, V.V. Plisko, K.N. Sukhushin, *in: Proc. IEEE Int. Pulsed Power Plasma Science Conf.*, 2001, pp. 1661–1664.

[6] E.G. Farr, C.E. Baum, W.D. Prather, L.H. Bowen, *in: Proc. Ultra-Wideband, Short-Pulse Electromagnetics 4*, 1999, pp. 131–144.